6(1): 33-41 (2021) https://doi.org/10.33484/sinopfbd.857418

Sinop Üniversitesi Fen Bilimleri Dergisi
Sinop Uni J Nat Sci

ISSN: 2536-4383
E-ISSN: 2564-4383

https://dergipark.org.tr/tr/pub/sinopfbd

Analysis of ^{9}Be Fusion Cross Sections via a Simple Cluster Model

Murat AYGUN[1]

How to cite: Aygun, M. (2021). Analysis of ^{9}Be fusion cross sections via a simple cluster model. *Sinop Üniversitesi Fen Bilimleri Dergisi*, *6*(1), 33-41. https://doi.org/10.33484/sinopfbd.857418

Research Article

Corresponding Author
Murat AYGUN
murata.25@gmail.com

ORCID of the Author
M.A.: 0000-0002-4276-3511

Received: 10.01.2021
Accepted: 26.04.2021

Abstract

The effects of different cluster configurations of ^{9}Be nucleus on the cross-sections of ^{9}Be + ^{28}Si, ^{9}Be + ^{64}Zn, ^{9}Be + ^{144}Sm, ^{9}Be + ^{186}W and ^{9}Be + ^{208}Pb fusion reactions have been explored for the first time using a simple cluster approach. The real potential has been calculated based on the α + α + n, d + ^{7}Li, ^{3}H + ^{6}Li, ^{3}He + ^{6}He and n + ^{8}Be cluster cases of the ^{9}Be nucleus while the imaginary potential is evaluated as Woods-Saxon potential. It has been seen that our results are in agreement with the experimental data. In addition to this, the fusion barrier height (V_B) and barrier position (R_B) values have been given for each reaction and cluster case.

Keywords: Cluster structure, fusion reactions, double folding model

Basit Bir Küme Modeli Aracılığıyla ^{9}Be Füzyon Tesir Kesitlerinin Analizi

[1]Bitlis Eren University, Faculty of Arts and Sciences, Department of Physics, 13000, Bitlis, Turkey

Öz

^{9}Be + ^{28}Si, ^{9}Be + ^{64}Zn, ^{9}Be + ^{144}Sm, ^{9}Be + ^{186}W ve ^{9}Be + ^{208}Pb füzyon reaksiyonlarının kesitleri üzerine ^{9}Be çekirdeğinin farklı küme konfigürasyonlarının etkileri basit bir küme yaklaşımı kullanılarak ilk kez araştırılmıştır. Sanal potansiyel Woods-Saxon potansiyeli olarak değerlendirilirken, reel potansiyel ^{9}Be çekirdeğinin α + α + n, d + ^{7}Li, ^{3}H + ^{6}Li, ^{3}He + ^{6}He ve n + ^{8}Be küme durumlarına göre hesaplanmıştır. Sonuçlarımızın deneysel verilerle uyumlu olduğu görülmüştür. Buna ek olarak füzyon bariyer yüksekliği (V_B) ve bariyer pozisyon (R_B) değerleri her bir reaksiyon ve küme durumu için verilmiştir.

Anahtar Kelimeler: Küme yapı, füzyon reaksiyonları, çift katlı model

Introduction

A cluster structure can be evaluated as a structure resulting from the movements of nucleons in a nucleus. Thus, a structure consisting of nucleons can be thought as one body [1]. In this respect, the ^{9}Be nucleus can be assumed as α + α + n, d + ^{7}Li, ^{3}H + ^{6}Li, ^{3}He + ^{6}He and n + ^{8}Be cluster structures [2–4] although the cluster structure of ^{9}Be is not known exactly yet [5]. Therefore, cluster structure is still a hot topic, and many studies can be found in the literature.

In recent years, Aygun has proposed a simple cluster method, and has performed the elastic scattering calculations of ^{9}Li [6], ^{9}Be [7], ^{12}Be [8], ^{12}B [9] and ^{22}Ne [10] nuclei. He has gotten the results compatible with the experimental data. However, this approach has not been applied to fusion cross-sections (FCSs). Therefore, we believe that it will be useful to

evaluate this approach in the theoretical analysis of fusion reactions.

We examine the effects of different cluster configurations of the ^{9}Be nucleus on the FCSs of ^{9}Be + ^{28}Si, ^{9}Be + ^{64}Zn, ^{9}Be + ^{144}Sm, ^{9}Be + ^{186}W and ^{9}Be + ^{208}Pb reactions over a simple cluster model. ^{9}Be with low binding energy and cluster structure is an important nucleus in the field of nuclear physics. Also, it has a usage area in the field of nuclear technology like thermonuclear devices [11, 12]. We first obtain the density distributions for α + α + n, d + ^{7}Li, ^{3}H + ^{6}Li, ^{3}He + ^{6}He and n + ^{8}Be cluster cases of the ^{9}Be nucleus. Then, we calculate the real potentials for each fusion reaction using these density distributions within a double folding (DF) model. We get the fusion cross-sections via the optical model (OM). Finally, we give fusion barrier height (V_B) and barrier position (R_B) values for each reaction and each cluster case.

Theoretical Formalism

Calculation Process

The total effective potential that is a significant parameter in the analysis of fusion reactions can be considered as

$$V_{Total}(r) = V_{Coulomb}(r) + \underbrace{\underbrace{V(r)}_{Real} + \underbrace{iW(r)}_{Imaginary}}_{V_{Nuclear}(r)} \quad (1)$$

$V_{Coulomb}(r)$ potential is given by [13]

$$V_{\text{Coulomb}}(r) = \frac{1}{4\pi\varepsilon_0}\frac{Z_P Z_T e^2}{r}, \qquad r \geq R_C$$

$$= \frac{1}{4\pi\varepsilon_0}\frac{Z_P Z_T e^2}{2R_C}\left(3-\frac{r^2}{R_C^2}\right), \quad r < R \quad (2)$$

$R_c = 1.25(A_P^{\frac{1}{3}} + A_T^{\frac{1}{3}})$.

The real potential is gotten for five cluster structures of ^{9}Be. Detailed information about these structures can be found in our previous study [7]. The calculations of the real potential are carried within the framework of the DF potential shown by

$$V_{\text{DF}}(\vec{r}) = \int d\vec{r}_1 \int d\vec{r}_2 \rho_P(\vec{r}_1)\rho_T(\vec{r}_2)\, v_{NN}(\vec{r}-\vec{r}_1+\vec{r}_2) \quad (3)$$

where $\rho_{P(T)}(\vec{r}_{1(2)})$, respectively are the densities of projectile (target). The densities of ^{28}Si, ^{186}W and ^{208}Pb targets are accepted in the two parameter Fermi (2pF) form, and the parameters are demonstrated in Table 1. On the other hand, the densities of ^{64}Zn and ^{144}Sm targets are supplied from RIPL-3 [14, 15].

Table 1. *2pF density parameters of the ^{28}Si, ^{186}W and ^{208}Pb nuclei*

Nucleus	***c***	***z***	***ρ₀***	**Ref.**
^{28}Si	3.15	0.475	0.175	[16]
^{186}W	6.58	0.480	0.148087	[17]
^{208}Pb	6.62	0.551	0.1600	[18]

The nucleon-nucleon interaction (v_{NN}) is parameterized by [13]

$$v_{NN}(r) = \gamma_1 \frac{e^{-\gamma_2 r}}{\gamma_2 r} - \gamma_3 \frac{e^{-\gamma_4 r}}{\gamma_4 r} - 276 \left(1 - 0.005 \frac{E_{Lab}}{A_p}\right) \delta(r) \text{ MeV} \quad (4)$$

where γ_1, γ_2, γ_3 and γ_4 are 7999 MeV, 4.0 fm^{-1}, 2134 MeV and 2.5 fm^{-1}, respectively. The imaginary potential is applied in the Woods-Saxon (WS) form

$$W(r) = -\frac{W_0}{1 + \exp\left(\frac{r - r_W (A_P^{\frac{1}{3}} + A_T^{\frac{1}{3}})}{a_W}\right)} \quad (5)$$

where W_0, r_w and a_w are the depth, radius, and diffuseness parameters, respectively. The codes DFPOT [19] and FRESCO [20] are used in the DF model and the cross-section calculations, respectively.

Results and Discussion

The total potential for the theoretical analysis of the fusion reactions has been calculated using Equation (1). According to this, the real potential has been acquired via the DF model by using the density distributions calculated for five different cluster cases of ^{9}Be. The imaginary potential has been taken as the WS potential. The appropriate values of WS potential have been researched and given in Table 2. Thus, we have plotted the total potential according to the distance in Figure 1.

Table 2. *The imaginary potential parameters (W_0, r_w and a_w) used in the theoretical analysis of ^{9}Be + ^{28}Si, ^{64}Zn, ^{144}Sm, ^{186}W and ^{208}Pb fusion reactions for α + α + n, d + ^{7}Li, ^{3}H + ^{6}Li, ^{3}He + ^{6}He and n + ^{8}Be cluster cases*

Reaction	**Parameter**	**α + α + n**	**d + ^{7}Li**	**^{3}H + ^{6}Li**	**^{3}He + ^{6}He**	**n + ^{8}Be**
	W_0 (MeV)	4.00	3.00	3.40	3.10	2.70
^{9}Be + ^{28}Si	r_w (fm)	0.82	0.82	0.82	0.82	0.82
	a_w (fm)	0.55	0.55	0.55	0.55	0.55
	W_0 (MeV)	12.8	15.0	16.2	12.8	12.8
^{9}Be + ^{64}Zn	r_w (fm)	1.27	1.27	1.27	1.27	1.27
	a_w (fm)	0.93	0.93	0.93	0.93	0.93
	W_0 (MeV)	11.3	11.7	10.1	7.30	3.30
^{9}Be + ^{144}Sm	r_w (fm)	1.27	1.27	1.27	1.27	1.27
	a_w (fm)	0.59	0.59	0.59	0.59	0.59
	W_0 (MeV)	3.00	2.50	2.60	2.30	1.70
^{9}Be + ^{186}W	r_w (fm)	0.87	0.87	0.87	0.87	0.87
	a_w (fm)	0.40	0.40	0.40	0.40	0.40
	W_0 (MeV)	5.60	4.80	4.80	3.60	2.40
^{9}Be + ^{208}Pb	r_w (fm)	0.87	0.87	0.87	0.87	0.87
	a_w (fm)	0.40	0.40	0.40	0.40	0.40

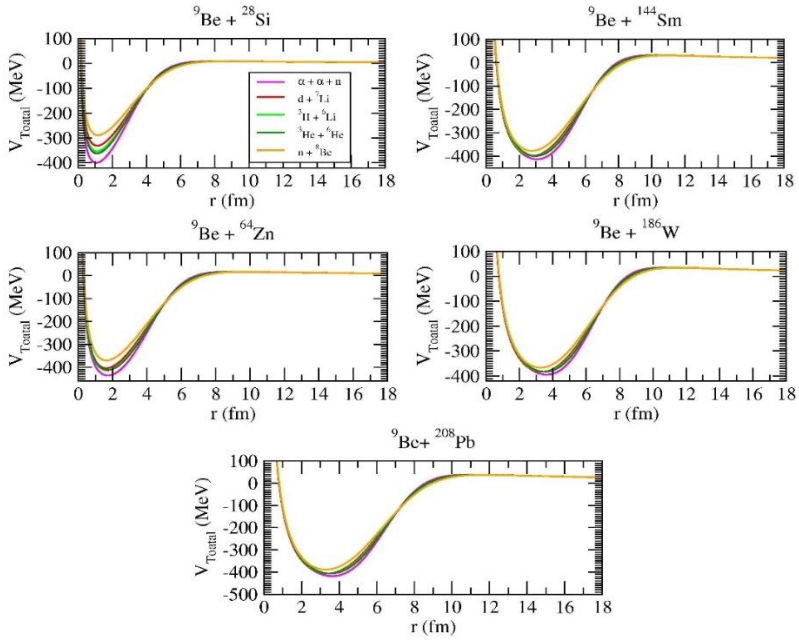

Figure 1. *The total potentials (in MeV) according to r (fm) for ^{9}Be + ^{28}Si, ^{64}Zn, ^{144}Sm, ^{186}W and ^{208}Pb fusion systems by using α + α + n, d + ^{7}Li, ^{3}H + ^{6}Li, ^{3}He + ^{6}He and n + ^{8}Be cluster cases*

As will be seen from Figure 1, the deepest potential for all reactions has been obtained for α + α + n cluster case. Accordingly, it means that this potential is more attractive than the potentials of the other cluster cases. In addition, it has been seen that the shallowest potential has been gotten for n + ^{8}Be. Finally, it has been observed that nuclear pocket width has increased as the nucleon number of target nucleus has increased.

Then, we have calculated the FCSs of ^{9}Be + ^{28}Si reaction for α + α + n, d + ^{7}Li, ^{3}H + ^{6}Li, ^{3}He + ^{6}He and n + ^{8}Be cluster cases of ^{9}Be. We have compared the results with the data in Figure 2. We have tracked that the α + α + n and ^{3}H + ^{6}Li results are very similar. However, we have noticed that the results of all cluster cases have shown an average behavior with the experimental data.

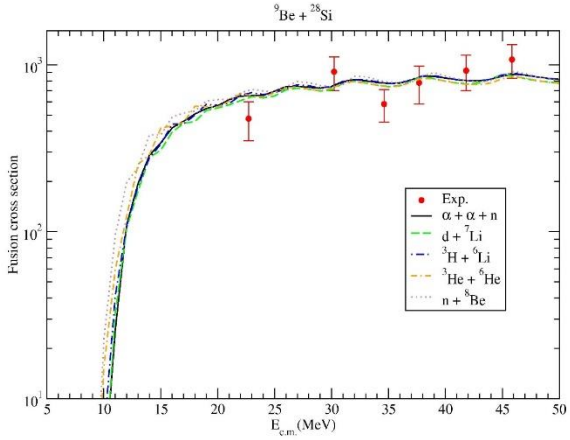

Figure 2. *The FCSs of ^{9}Be + ^{28}Si reaction calculated using α + α + n, d + ^{7}Li, ^{3}H + ^{6}Li, ^{3}He + ^{6}He and n + ^{8}Be cluster cases. The data is from [21]*

We have obtained the FCSs of ^{9}Be + ^{64}Zn reaction for the same cluster structures. We have compared the theoretical results with the data in Figure 3. We have realized that the results are generally similar to each other, and display good consistent with the data.

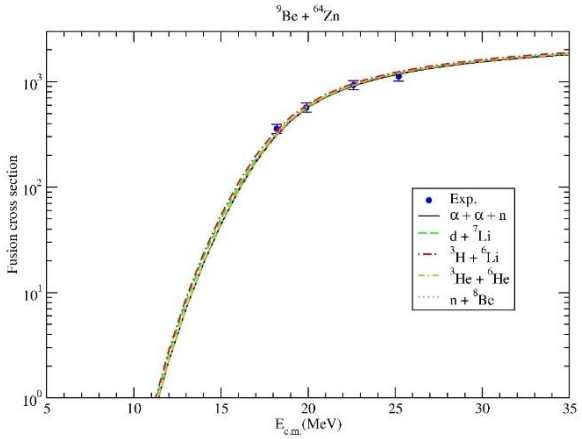

Figure 3. *The same Figure 2, but for ^{9}Be + ^{64}Zn fusion reaction. The data is from [22]*

Then, we have acquired the FCSs of ^{9}Be + ^{144}Sm reaction for five different cluster cases. We have showed our results together with the data in Figure 4. We have monitored that the cluster results are different from each other at small angles while they are very close at further angles. Additionally, we can say that their compatibility with the data is good.

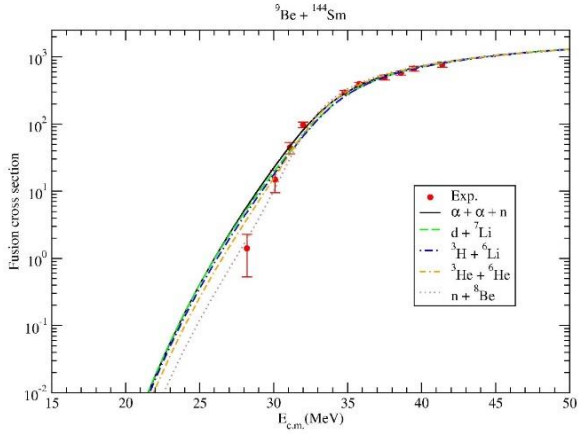

Figure 4. *The same Figure 2, but for ^{9}Be + ^{144}Sm fusion reaction. The data is from [23]*

We have gotten the FCSs of ^{9}Be + ^{186}W reaction for various cluster cases of the ^{9}Be nucleus. We have compared the results with the data in Figure 5. We have experienced that the cluster cases are very close to each other at forward angles, and are in good agreement with the data in general sense. Additionally, we have observed that n + ^{8}Be cluster case is slightly better than the other cluster cases.

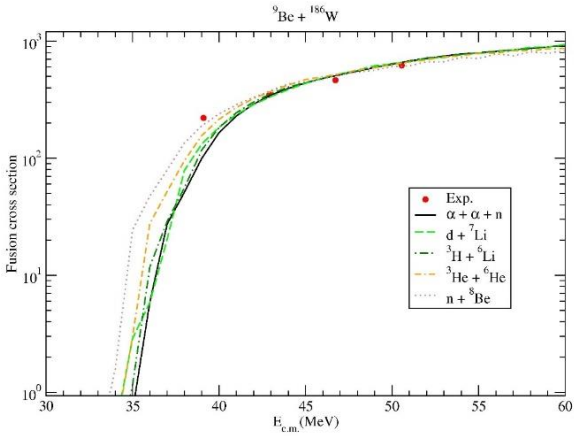

Figure 5. *The same Figure 2, but for ^{9}Be + ^{186}W fusion reaction. The data is from [24]*

Finally, we have calculated the FCSs of ^{9}Be + ^{208}Pb reaction for α + α + n, d + ^{7}Li, ^{3}H + ^{6}Li, ^{3}He + ^{6}He and n + ^{8}Be cluster cases of ^{9}Be. We have compared our results and the data in Figure 6. We have observed that the d + ^{7}Li and ^{3}H + ^{6}Li cluster cases are very close to each other. Also, we have noticed that other cluster results, except for n + ^{8}Be cluster case, have shown an average behavior with the data. However, we have observed that the compatibility of n + ^{8}Be result with the data is very good, and is much better than the other cluster results.

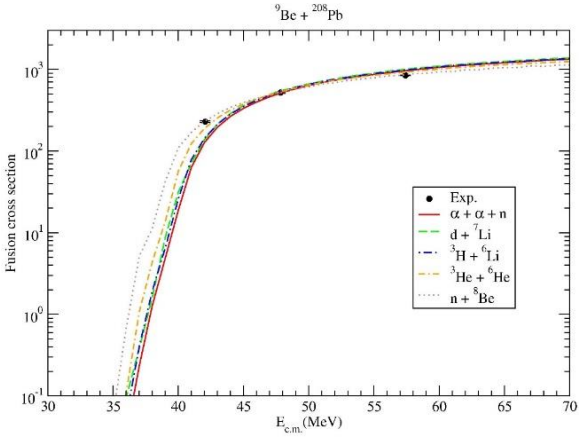

Figure 6. *The same Figure 2, but for ^{9}Be + ^{208}Pb fusion reaction. The data is from [25]*

In the present study, we have also calculated the fusion barrier height (V_B) and barrier position (R_B) for each reaction and each cluster case. They are known as basic parameters in defining nuclear fusion reactions. We have listed all the values of V_B and R_B in Table 3. We have obtained the highest R_B value and the lowest V_B value for n + ^{8}Be cluster case in all the reactions. In addition to this, we have found for α + α + n cluster case the highest V_B value except for ^{9}Be + ^{28}Si and ^{9}Be + ^{64}Zn reactions and the lowest R_B value in all the reactions. Thus, it can be said that the kinetic energy of the projectile for n + ^{8}Be cluster state can be less than the other cluster states.

Table 3. *The fusion barrier heights (V_B) and positions (R_B) calculated based on the theoretical analysis of ^{9}Be + ^{28}Si, ^{64}Zn, ^{144}Sm, ^{186}W and ^{208}Pb fusion reactions for α + α + n, d + ^{7}Li, ^{3}H + ^{6}Li, ^{3}He + ^{6}He and n + ^{8}Be cluster cases*

Reaction	Parameter	α + α + n	d + ^{7}Li	^{3}H + ^{6}Li	^{3}He + ^{6}He	n + ^{8}Be
^{9}Be + ^{28}Si	V_B (MeV)	8.67	8.86	8.76	8.40	8.24
	R_B (fm)	8.15	8.44	8.40	8.58	8.84
^{9}Be + ^{64}Zn	V_B (MeV)	17.05	17.17	17.07	16.55	16.20
	R_B (fm)	9.04	9.38	9.30	9.42	9.72
^{9}Be + ^{144}Sm	V_B (MeV)	31.66	31.59	31.52	30.80	30.15
	R_B (fm)	10.24	10.60	10.52	10.58	10.92
^{9}Be + ^{186}W	V_B (MeV)	35.92	35.83	35.76	35.01	34.30
	R_B (fm)	10.82	11.20	11.10	11.16	11.50
^{9}Be + ^{208}Pb	V_B (MeV)	38.98	38.86	38.82	38.09	37.31
	R_B (fm)	11.06	11.40	11.32	11.38	11.70

Conclusions

We have calculated the FCSs of ^{9}Be + ^{28}Si, ^{9}Be + ^{64}Zn, ^{9}Be + ^{144}Sm, ^{9}Be + ^{186}W and ^{9}Be + ^{208}Pb reactions for the α + α + n, d + ^{7}Li, ^{3}H + ^{6}Li, ^{3}He + ^{6}He and n + ^{8}Be cluster structures of ^{9}Be. We have compared the theoretical results with the experimental data. We have obtained agreement results with the data. We have also given the fusion barrier height and barrier position for each reaction and each cluster case.

Consequently, we have provided new results on various fusion reactions of ^{9}Be over a simple

cluster approach. We think that this approach will be useful to apply to other fusion reactions.

Acknowledgments -

Funding/Financial Disclosure The author has no received any financial support for the research, or publication of this study.

Ethics Committee Approval and Permissions -

Conflict of Interests -

Authors Contribution Author read and approved the final manuscript.

References

[1] Urazbekov, B. A., Denikin, A. S., Lukyanov, S. M., Itaco, N., Janseitov, D. M., Mendibayev, K., Burjan, V., Kroha, V., Mrazek, J., Trzaska, W. H., Harakeh, M. N., Etasse, D., Stefan, I., Verney, D., Issatayev, T., Penionzhkevich, Yu E., Kuterbekov, K. A., & Zholdybaye, T. (2019). Clusterization and strong coupled-channels effects in deuteron interaction with ^{9}Be nuclei. *Journal of Physics G: Nuclear and Particle Physics, 46*(10), 105-110. https://doi.org/10.1088/1361-6471/ab37a6

[2] Lukyanov, S. M., Harakeh, M. N., Naumenko, M. A., Xu Yi, Trzaska, W. H., Burjan, V., Kroha, V., Mrazek, J., Glagole, V., Piskoř, Š., Voskoboynik, E. I., Khlebnikov, S. V., Penionzhkevich, YuE, Skobelev, N. K., Sobolev, G., Yu., Tyurin, G. P., Kuterbekov, K., & Tuleushev, Yu. (2015). Some insights into cluster structure of ^{9}Be from ^{3}He + ^{9}Be reaction. *World Journal of Nuclear Science and Technology, 5*(4), 265-273. https://doi.org/10.4236/wjnst.2015.54026

[3] Camacho, A. G., Gomes, P. R. S., Lubian, J., & Padrón, I. (2008). Simultaneous optical model analysis of elastic scattering, fusion, and breakup for the ^{9}Be + ^{144}Sm system at near-barrier energies. *Physical Review C, 77*(5), Article 054606. https://link.aps.org/doi/10.1103/PhysRevC.77.054606

[4] Sert, Y., Yegin, R., & Doğan, H. (2015). A theoretical investigation of ^{9}Be+ ^{27}Al reaction: phenomenological and microscopic model approximation. *Indian Journal of Physics, 89*(10), 1093-1100. https://doi.org/10.1007/s12648-015-0685-9

[5] Pandit, S. K., Jha, V., Mahata, K., Santra, S., Palshetkar, C. S., Ramachandran, K., Parkar, V. V., Shrivastava, A., Kumawat, H., Roy, B. J., Chatterjee, A., & Kailas, S. (2011). Investigation of cluster structure of ^{9}Be from high precision elastic scattering data. *Physical Review C, 84*(3), Article 031601. https://link.aps.org/doi/10.1103/PhysRevC.84.031601

[6] Aygun, M. (2017). A comparative analysis of the density distributions and the structure models of ^{9}Li. *Pramana, 88*(3), Article 53. https://doi.org/10.1007/s12043-016-1360-1

[7] Aygun, M., & Aygun, Z. (2017). A theoretical study on different cluster configurations of the ^{9}Be nucleus by using a simple cluster model. *Nuclear Science and Techniques, 28*(6), Article 86. https://doi.org/10.1007/s41365-017-0239-2

[8] Aygun, M. (2016). A comprehensive study on the internal structure and thedensity distribution of ^{12}Be. *Revista Mexicana de Física, 62*(4), 336-343. http://www.redalyc.org/articulo.oa?id=57046490009

[9] Aygun, M. (2020). A comprehensive theoretical analysis of ^{12}B + ^{58}Ni elastic scattering measured for the first time by using different density distributions, different nuclear potentials and different cluster approaches. *Pramana, 94*(1), 1-14. https://doi.org/10.1007/s12043-020-01979-w

[10] Aygun, M. (2020). A comprehensive theoretical analysis of ^{22}Ne nucleus by using different density distributions, different nuclear potentials and different cluster approach. *International Journal of Modern Physics E, 29*(01), Article 1950112. https://doi.org/10.1142/S021830131950112X

[11] Kukulin, V. I., & Voronchev, V. T. (2010). Pinch-based thermonuclear D 3 He fusion driven by a femtosecond laser. *Physics of Atomic Nuclei, 73*(8), 1376-1383. https://doi.org/10.1134/S1063778810080107

[12] Seksembayev, Z., Kukulin, V., & Sakhiyev, S. (2018). Study of a dense hot plasma's burning in Z-pinch devices with inertial-magnetic confinement. *Physica Scripta, 93*(8), Article 085602. https://doi.org/10.1088/1402-4896/aacadf

[13] Satchler, G. R., & Love, W. G. (1979). Folding model potentials from realistic interactions for heavy-ion scattering. *Physics Reports, 55*(3), 183-254. https://doi.org/10.1016/0370-1573(79)90081-4

[14] RIPL-3 (2021, May 23). Reference Input Parameter Library. http://www-nds.iaea.org/RIPL-3.

[15] Capote, R., Herman, M., Obložinský, P., Young, P. G., Goriely, S., Belgya, T., Ignatyuk, A. V., Koning, A. J., Hilaire, S., Plujko, V. A., Avrigeanu, M., Bersillon, O., Chadwick, M. B., Fukahori, T., Ge, Z., Han, Y., Kailas, S., Kopecky, J., Maslov, V. M., Reffo, G., Sin, M., Soukhovitskii, E. Sh., & Talou, P. (2009). RIPL–reference input parameter library for calculation of nuclear reactions and nuclear data evaluations. *Nuclear Data Sheets, 110*(12), 3107-3214. https://doi.org/10.1016/j.nds.2009.10.004

[16] Farid, M. E. A., & Hassanain, M. A. (2000). Density-independent folding analysis of the ^{6,7}Li elastic scattering at intermediate energies. *Nuclear Physics A, 678*(1-2), 39-75. https://doi.org/10.1016/S0375-9474(00)00313-4

[17] De Jager, C. W., De Vries, H., & De Vries, C. (1974). Nuclear charge-and magnetization-density-distribution parameters from elastic electron scattering. *Atomic Data and Nuclear Data Tables, 14*(5-6), 479-508. https://doi.org/10.1016/S0092-640X(74)80002-1

[18] Hossain, S., Abdullah, M. N. A., Rahman, M. Z., Basak, A. K., & Malik, F. B. (2013). Non-monotonic potentials for ^{6}Li elastic scattering at 88 MeV. *Physica Scripta, 87*(1), Article 015201. https://doi.org/10.1088/0031-8949/87/01/015201

[19] Cook, J. (1982). DFPOT-a program for the calculation of double folded potentials. *Computer Physics Communications, 25*(2), 125-139.

[20] Thompson, I. J. (1988). Coupled reaction channels calculations in nuclear physics. *Computer Physics Reports, 7*(4), 167-212. https://doi:10.1016/0167-7977(88)90005-6

[21] Eck, J. S., Leigh, J. R., Ophel, T. R., & Clark, P. D. (1980). Total fusion cross section for the ^{9}Be + ^{28}Si system. *Physical Review C, 21*(6), Article 2352. https://doi.org/10.1103/PhysRevC.21.2352

[22] Moraes, S. B., Gomes, P. R. S, Lubian, J., Alves, J. J. S., Anjos, R. M., SantAnna, M. M., Padrn, I., Muri, C., Liguori, Neto, R., & Added, N. (2000). Fusion and elastic scattering of ^{9}Be+ ^{64}Zn: a search of the breakup influence on these processes. *Physical Review C, 61*(6), Article 064608. https://doi.org/10.1103/PhysRevC.61.064608

[23] Gomes, P. R. S., Padron, I., Crema, E., Capurro, O., Fernández, Niello, J. O., Arazi, A., Martí, G.V., Lubian, J., Trotta, M., Pacheco, A., Testoni, J. E., Rodríguez, M. D., Ortega, M. E., Chamon, L., Anjos, R.M., Veiga, R., Dasgupta, M., Hinde, D. J., & Hagino, K. (2006). Comprehensive study of reaction mechanisms for the ^{9}Be + ^{144}Sm system at near-and sub-barrier energies. *Physical Review C, 73*(6), Article 064606. https://doi.org/10.1103/PhysRevC.73.064606

[24] Kharab, R., & Kumari, A. (2019). Influence of projectile breakup on fusion reactions induced by ^{9}Be at near barrier energies. *Nuclear Physics A, 981*, 62-74. https://doi.org/10.1016/j.nuclphysa.2018.10.081

[25] Dasgupta, M., Hinde, D. J., Sheehy, S. L., & Bouriquet, B. (2010). Suppression of fusion by breakup: Resolving the discrepancy between the reactions of ^{9}Be with ^{208}Pb and ^{209}Bi. *Physical Review C, 81*(2), Article 024608. https://doi.org/10.1103/PhysRevC.81.024608